Danuta Lipa
Institute of Geological Sciences, University of Wrocław

Jacek Puziewicz
Institute of Geological Sciences, University of Wrocław

Theodoros Ntaflos
Department of Lithospheric Research, University of Vienna

Magdalena Matusiak-Małek
Institute of Geological Sciences, University of Wrocław

Clinopyroxene megacrysts from basanite of Ostrzyca Proboszczowicka in Lower Silesia (SW Poland)

Abstract

Cenozoic basanite forming the Ostrzyca Proboszczowicka Hill in SW Poland contains 1.5 — 3.0 cm long clinopyroxene "megacrysts." They contain intergrowths of euhedral apatite (up to 7 mm long) and older clinopyroxene grains. The megacrysts have the composition of aluminian-sodian diopside (Mg# 0.61–0.70), their REE contents are slightly (1–10 x) greater than those of primitive mantle. The REE patterns of megacrysts are enriched in light REE relative to heavy REE. Trace element patterns exhibit strong positive Zr, Hf and Ta anomalies and pronounced negative Sr and Ti anomalies. Apatite has composition of fluor-apatite. The REE concentrations in apatite reach up to 1000 x primitive mantle values for LREE, while trace element patterns are characterized by strong negative anomalies of HFSE and Pb. Megacrysts come from the not solidified coarse-grained cumulate, which was formed at mid-crustal level from the fractionated silicate alkaline magma batch. The new pulse of primitive basanitic magma entrained the megacrysts and brought them to the surface.

Streszczenie

W obrębie kenozoicznego bazanitu budującego wzgórze Ostrzyca Proboszczowicka (SW Polska) występują liczne „megakryształy" klinopiroksenu osiągające długość od 1,5 do 3 cm. Megakryształy zawierają wrostki euhedralnego apatytu (długości do 7 mm) i starszego klinopiroksenu. Klinopiroksen tworzący megakryształy ma skład glinowo-sodowego diopsydu (mg# 0,61–0,70) a zawartość

REE jest nieznacznie (1–10 razy) wyższa od ich zawartości w prymitywnym płaszczu. Diagramy pajęcze dla REE wykazują wzbogacenie w lekkie ziemie rzadkie. Klinopiroksen wykazuje pozytywne anomalie zawartości Zr, Hf i Ta oraz negatywne anomalie zawartości Sr i Ti. Apatyt ma skład apatytu fluorowego i jest silnie wzbogacony w pierwiastki ziem rzadkich (do 1000 wartości w prymitywnym płaszczu). Apatyt wykazuje silne negatywne anomalie w zawartości HFSE i Pb. Megakryształy klinopiroksenu pochodzą z niekonsolidowanego, gruboziarnistego kumulatu, który wykrystalizował ze sfrakcjonowanej magmy alkalicznej na głębokościach opowiadających środkowej skorupie. Nowy puls prymitywnej magmy bazanitowej spowodował dezintegrację kumulatu i wyniósł jego fragmenty na powierzchnię.

Keywords: clinopyroxene, megacryst, basanite, Cenozoic, Ostrzyca Proboszczowicka, SW Poland

Introduction

The clinopyroxene megacrysts occur worldwide in the alkaline basalts and have pheno- or xenocrystic nature (for review see e.g. Woodland and Jugo 2007 and references therein). The megacrysts, which usually are from few to ten centimetres long, occur also in some alkaline basaltic lavas belonging to the Polish part of the Cenozoic Central European Volcanic Province (SW Poland). They have been reported from mantle peridotite xenoliths-bearing lavas: nephelinite from Księginki (Białowolska 1980; Kozłowska-Koch 1981; Puziewicz et al. 2011), basanite from Lutynia/Lądek Zdrój (Kozłowska-Koch 1976; Białowolska 1980; Bakun-Czubarow and Białowolska 2001; Matusiak-Małek 2010) and basanite from Krzeniów (Trupień Hill; Białowolska 1980). The megacrysts occur also in the xenolith-free basanite from the Ostrzyca Proboszczowicka Hill near Złotoryja. Since they have never been characterised in detail, in this paper we present their textural and chemical description.

Geological setting

The Cenozoic alkaline lavas occur in SW Poland, forming the north-eastern part of the Central European Volcanic Province (CEVP; for details see Wilson and Downes 2006). The Late Cretaceous to Cenozoic CEVP extends from the Massif Central in France, through the Rhenish Massif in Germany to the Bohemian Massif in Czech Republic and Poland. The volcanic rocks are related to episodes of rifting, which affected the Variscan Platform during the Alpine orogeny (Ulrych et al. 1999). The volcanism results from small-scale diapirs melt which originated from decompressional melting of lithospheric mantle (Wilson and Downes 2007). The Polish Cenozoic lava occurrences are concentrated at the NE termination of the Eger (Ohře) Graben and

to the SE of it, where they are considered to be related to the Labe-Odra fault system (Ulrych et al. 2011). The Cenozoic volcanic rocks in Lower Silesia form five "volcanic complexes": Lubań-Frydlant, Złotoryja-Jawor, Niemcza-Strzelin, Lądek Zdrój and Niemodlin (Figure 1). The Ostrzyca Proboszczowicka basanite (Szumowska 2013; Szumowska et al. 2013) belongs to the Złotoryja-Jawor complex (Figure 1). The basanite forms neck (Szumowska et al. 2013), probably of Miocene age (Birkenmajer et al. 2007), surrounded by Lower Permian conglomerates and sandstones (Milewicz and Kozdrój 1995).

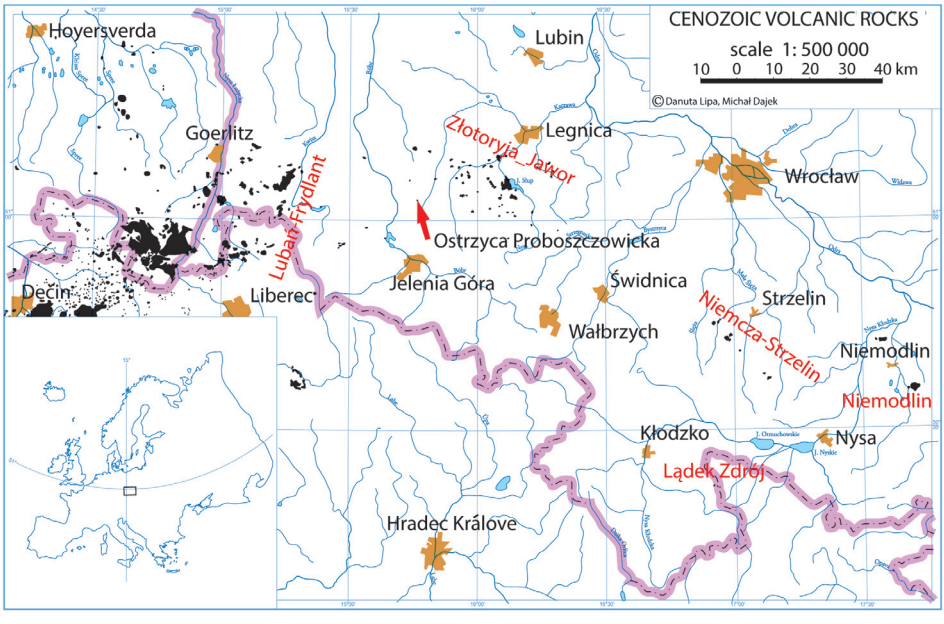

Figure 1. Location of the Ostrzyca Proboszczowicka relative to occurrences of Cenozoic alkaline basaltic rocks in SW Poland. Outcrops of Cenozoic alkaline volcanic rocks in SW Poland and neighbouring areas of Germany and Czech Republic. "Volcanic complexes" after Puziewicz et al. (2015). Compiled by M. Dajek and D. Lipa from Sawicki (1995)

Analytical methods

Eleven rock samples containing clinopyroxene megacrysts were collected from boulders near the peak of Ostrzyca Proboszczowicka. Chemical composition of megacrysts was studied in 8 thick (100 μm) sections using CAMECA SX-100 electron microprobe working under standard conditions (accelerating voltage 15 kV, beam current 20 nA, beam diameter 1 μm) in the laboratory of Department für Litosphärenforschung, Universität Wien, Austria. The content of trace elements was determined in 7 thick sections (103 points) using the LA-ICP-MS Laboratory in the Institute of Geological

Sciences, Polish Academy of Science, Cracow, Poland. Analyses of clinopyroxene were performed at a beam diameter of 155 microns, frequency of 10 Hz, and those of apatite at beam diameter of 60 microns and the time of ablation extended to 75 s for apatite crystals. NIST 612 and GOR 128-G were used as external standards for clinopyroxene megacrysts, NIST 612, MPI1 (DL3310) and MPI2 (DL3302) for apatite. The Ca content determined by electron microprobe was used as an internal standard. Further analytical details are reported in Matusiak-Małek et al. (2014). Bulk-rock chemical XRF analyses of host basanite (5 samples) were done in the laboratory of Department für Litosphärenforschung, Universität Wien, Austria.

In the article we have used abbreviations: "Mg#" referring to $Mg/(Mg+Fe^{tot})$ ratio, "a pfu" referring to "atoms per formula unit", and "PM" referring to elements concentrations in primitive mantle sensu McDonough and Sun (1995).

Megacryst's texture and mineral chemistry

Megacrysts of clinopyroxene are black, up to 3 cm long (Figure 2), have anhedral shapes with singular euhedral faces. Some of the megacrysts are elongated, while others have rounded shapes.

Figure 2. Appearance of the clinopyroxene megacryst in host basanite on the Ostrzyca Proboszczowicka Hill. Coin diameter is 2 cm

In the thick section clinopyroxene megacrysts are pleochroic (green to yellow). Some surfaces are covered by yellowish, 0.5–2 mm thick reaction fringe formed by subhedral clinopyroxene (Figure 3). Megacrysts consist of domains differing by colour intensity (darker and lighter). All of the investigated samples reveal sector-zoning (except DL3303) and in one case (DL3308) internal-zoning is observed. Megacrysts are fractured, in some specimens trails of inclusions occur. The 5 mm long, pleochroic (yellow to green) euhedral intergrowths

of older clinopyroxene grains were identified in two megacrysts (DL3302 and DL3307; Figure 3).

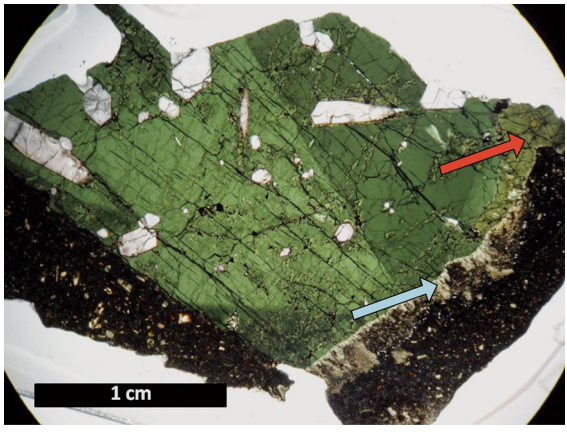

Figure 3. Example of studied clinopyroxene megacryst DL3302 in plane polarized light. The sample consists of domains with inclusions of apatite and older diopside (red arrow). On the preserved faces the yellowish fringe is observed (blue arrow)

The central parts of megacrysts have the composition of iron-rich diopside, while fringes contain more Ca and Mg and has the composition of subsilicic diopside and diopside (Figure 4).

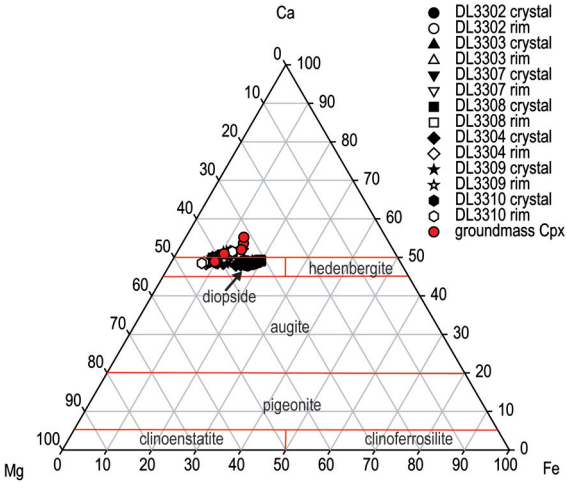

Figure 4. Mg-Fe-Ca pyroxene classification diagram (Morimoto 1989) illustrating the compositional variations between core areas of the megacrysts (black), reaction fringe (white) and basanite groundmass clinopyroxene (red)

The Mg# of the megacrysts ranges from 0.61 to 0.70 (Tables 1, 2, 3). They contain significant sodium (Figure 5a), are Cr-free (Figure 5b) and Ti-poor (Figure 5c). The Ca content varies from 0.88 to 0.93 a pfu (Figure 5d), that of Al from 0.13 to 0.27 a pfu (Figure 5e, Table 2), Ti content ranges from 0.02 to 0.05 a pfu, while Na varies from 0.08 to 0.12 a pfu (Table 3). The Mg# is negatively correlated with Al, Ti and Na. The composition of sectors of different colours differs: darker domains reveal higher Al, Fe, Na and Ti content, lower Si, Mg and Ca content and lower Mg# compared to the lighter domains (Figure 6, Tables 1–4).

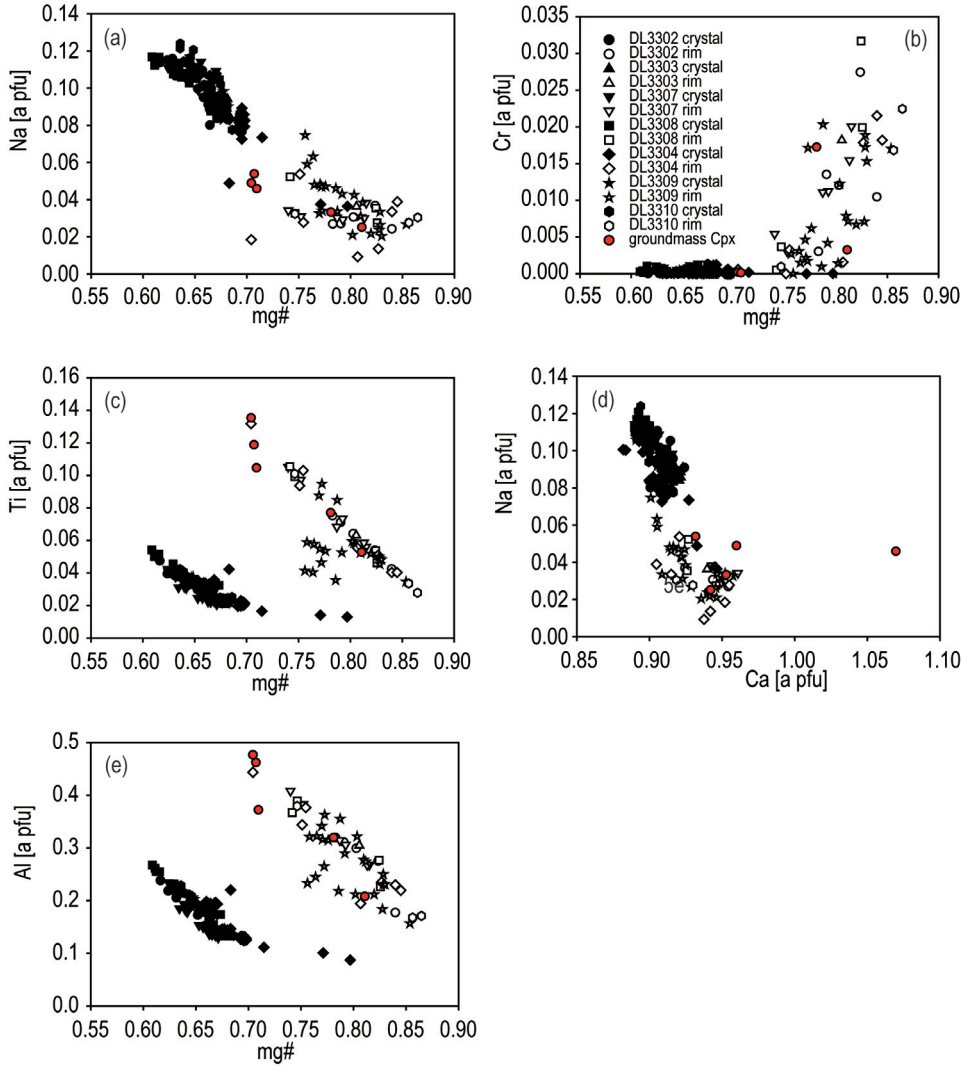

Figure 5. Diagrams illustrating chemical composition of clinopyroxene megacrysts from Ostrzyca Proboszczowicka (black) and their reaction fringes (white): (a) Mg# vs Na, (b) Mg# vs Cr, (c) Mg# vs Ti, (d) Ca vs Na, (e) Mg# vs Al. Legend as in Figure 4

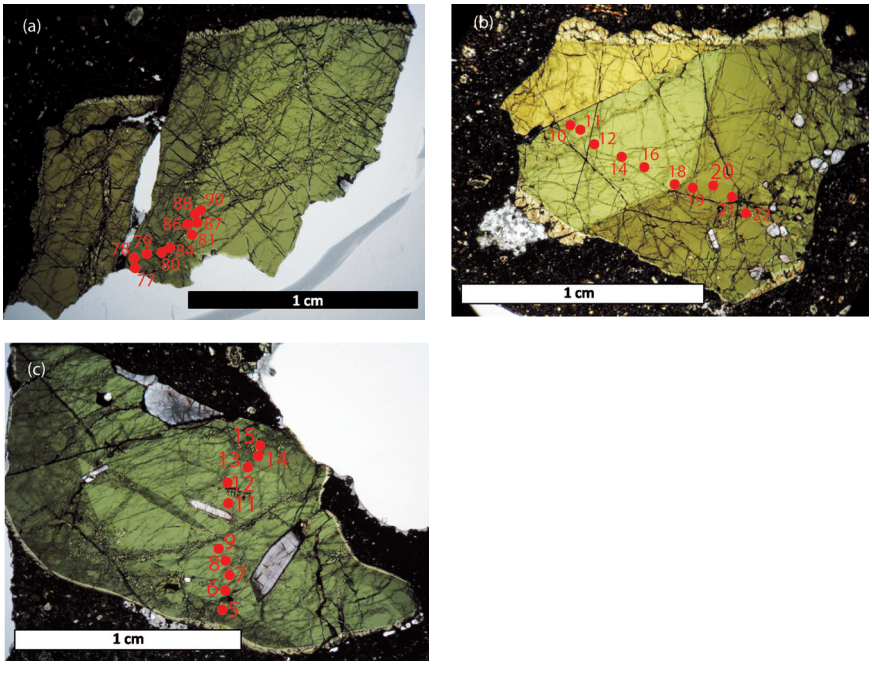

Figure 6. Location of major element analyses of the representative clinopyroxene megacrysts from Ostrzyca Proboszczowicka: (a) DL3304, (b) DL3308, (c) DL3310. Red points refer to analyses presented in Tables 1, 2 and 3

The composition of reaction fringes differs from the composition of megacrysts in terms of major elements: Ca is from 0.90 to 0.96 a pfu, Al from 0.16 to 0.44 a pfu, Ti from 0.03 to 0.13 a pfu, Cr to 0.03 a pfu, Na from 0.01 to 0.07 a pfu, Fe from 0.13 to 0.26 a pfu, Mg from 0.61 to 0.84 a pfu (Figure 5). Their Mg# varies from 0.70 to 0.86 (Table 4).

Primitive-mantle normalized REE patterns of the studied megacrysts are very similar and show enrichment in Light Rare Earth Elements (LREE) reaching up to 18 times primitive mantle value at Nd (Figure 7a, Table 5 and 6). The REE patterns of all the megacrysts show deflection in La-Nd (see Figure 7a). The trace element composition is characterized by positive Zr, Hf and in some cases also Ta anomalies, and negative U, La, Sr, Ti and Pb anomalies (Figure 7b). In some samples strong depletion (down to 0.01 x PM) in Rb and Ba is observed. The clinopyroxene forming fringes is enriched in REE (especially in LREE) and trace elements relative to the megacrysts, but lacks positive Zr and Hf anomalies (Figure 7a, b, Table 7).

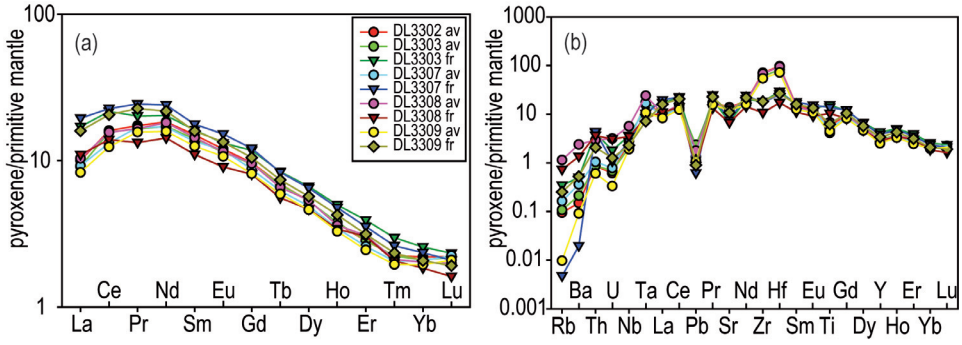

Figure 7. Primitive mantle (McDonough & Sun 1995) normalized REE (a) and trace element (b) patterns of the clinopyroxene megacrysts from Ostrzyca Proboszczowicka (circles; 'av' in the legend) and their reaction fringes (triangles; 'fr' in the legend)

Inclusions of apatite occur in three of the studied megacrysts (DL3302, DL3308 and DL3310). Their length reaches 7 mm. Apatite is transparent, with euhedral (prismatic) or anhedral shapes, usually fractured. Apatite has composition of fluor-apatite with F content ranging from 0.87 to 1.93 wt.%. Chlorine content is strongly variable between grains (0.05–1.75 wt.%); within single grain it is typically constant, but significant enrichment in Cl may occur at grain boundaries. Apatite is strongly enriched in in LREE (about 1000 x PM for LREE and about 10 x PM for HREE, Table 8 and 9). The REE patterns are nearly linear, with slight positive Nd and Gd anomalies (Figure 8a). The trace element patterns are characterized by very strong negative anomalies of HFSE (Nb, Ta, Zr, Hf, Ti) and Pb, and weaker negative Sr anomaly (Figure 8b). Concentration of Yb and Lu is on the level 10 x PM and La, Ce, Pr and Nd is near 1000 x PM, whereas Rb, Hf and Ti reveal depletion.

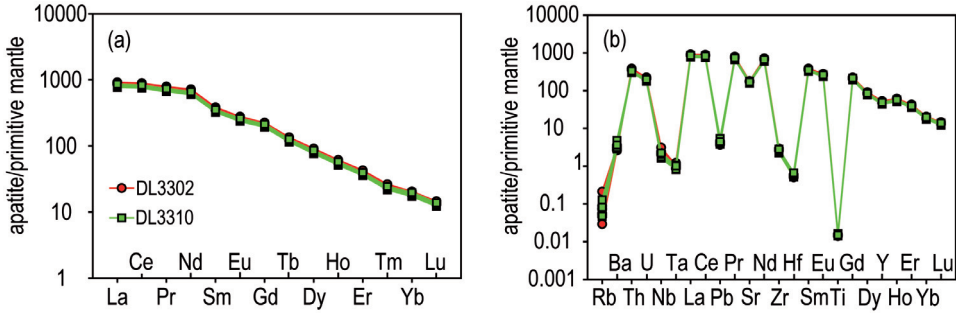

Figure 8. Primitive mantle (McDonough & Sun 1995) normalized REE (a) and trace element (b) patterns of apatite inclusions in clinopyroxene megacrysts from Ostrzyca Proboszczowicka

Table 1. Representative chemical analyses and structural formulae (O^{2-} = 6) of clinopyroxene megacryst DL3304 from the Ostrzyca Proboszczowicka (see Fig. 6a).

Analysis no.	77 / 1.	78 / 1.	79 / 1.	80 / 1.	81 / 1.	84 / 1.	86 / 1.	87 / 1.	88 / 1.	90 / 1.
SiO_2	48.99	49.12	48.98	49.16	50.43	47.93	49.26	50.50	50.61	50.60
TiO_2	1.16	1.16	1.19	1.26	0.70	1.48	1.10	0.76	0.78	0.73
Al_2O_3	4.31	4.33	4.31	4.39	2.90	4.90	4.19	2.83	2.94	2.93
Cr_2O_3	0.00	0.02	0.00	0.01	0.01	0.01	0.00	0.00	0.00	0.00
FeO*	9.96	10.02	9.81	9.89	9.30	9.58	10.11	9.42	9.29	9.22
MnO	0.24	0.27	0.23	0.27	0.29	0.25	0.28	0.28	0.24	0.26
NiO	0.02	0.00	0.01	0.00	0.00	0.00	0.00	0.00	0.00	0.00
MgO	11.05	11.10	11.19	11.20	11.90	11.59	11.14	11.91	11.94	11.88
CaO	22.10	21.96	22.19	21.96	22.31	22.83	21.63	22.18	22.31	22.33
Na_2O	1.45	1.35	1.46	1.43	1.21	0.66	1.36	1.11	1.14	1.17
Total	99.24	99.33	99.39	99.54	99.00	99.23	99.05	98.98	99.21	99.07
Si	1.87	1.87	1.86	1.87	1.92	1.83	1.88	1.92	1.92	1.92
Ti	0.03	0.03	0.03	0.04	0.02	0.04	0.03	0.02	0.02	0.02
Al	0.19	0.19	0.19	0.20	0.13	0.22	0.19	0.13	0.13	0.13
Cr	0.00	0.00	0.00	0.00	0.00	0.00	0.00	0.00	0.00	0.00
Fe^{2+}	0.32	0.32	0.31	0.31	0.30	0.31	0.32	0.30	0.29	0.29
Mn	0.01	0.01	0.01	0.01	0.01	0.01	0.01	0.01	0.01	0.01
Ni	0.00	0.00	0.00	0.00	0.00	0.00	0.00	0.00	0.00	0.00
Mg	0.63	0.63	0.64	0.63	0.67	0.66	0.63	0.67	0.67	0.67
Ca	0.90	0.90	0.90	0.89	0.91	0.93	0.88	0.90	0.91	0.91
Na	0.11	0.10	0.11	0.11	0.09	0.05	0.10	0.08	0.08	0.09
Total	4.06	4.05	4.06	4.05	4.04	4.05	4.05	4.04	4.04	4.04
Mg#	0.66	0.66	0.67	0.67	0.70	0.68	0.66	0.69	0.70	0.70

* Total Fe as FeO

Table 2. Representative chemical analyses and structural formulae (O^{2-} = 6) of clinopyroxene megacryst DL3308 from the Ostrzyca Proboszczowicka (see Fig. 6b).

Analysis no. no.	10 / 1 .	11 / 1 .	12 / 1 .	14 / 1 .	16 / 1 .	18 / 1 .	19 / 1 .	20 / 1 .	21 / 1 .	22 / 1.
SiO_2	49.62	49.70	49.88	50.24	50.15	49.71	47.26	47.15	47.16	46.91
TiO_2	0.97	0.91	0.84	0.86	0.82	0.92	1.75	1.79	1.74	1.87
Al_2O_3	3.67	3.38	3.18	3.03	3.00	3.45	5.64	5.62	5.77	5.89
Cr_2O_3	0.00	0.03	0.01	0.00	0.03	0.01	0.01	0.03	0.01	0.01
FeO*	10.17	10.19	10.02	10.06	9.88	10.16	11.15	11.04	11.24	11.21
MnO	0.29	0.28	0.28	0.27	0.28	0.24	0.26	0.29	0.28	0.24
NiO	0.01	0.01	0.02	0.00	0.00	0.00	0.02	0.00	0.03	0.01
MgO	11.20	11.34	11.37	11.51	11.61	11.40	9.87	9.90	9.91	9.78
CaO	22.41	22.44	22.33	22.56	22.42	22.38	21.89	21.79	21.62	21.62
Na_2O	1.35	1.22	1.23	1.14	1.15	1.26	1.52	1.57	1.51	1.57
Total	99.67	99.53	99.18	99.63	99.34	99.51	99.38	99.19	99.26	99.12
Si	1.89	1.89	1.90	1.91	1.91	1.89	1.81	1.81	1.81	1.81
Ti	0.03	0.03	0.02	0.02	0.02	0.03	0.05	0.05	0.05	0.05
Al	0.16	0.15	0.14	0.14	0.13	0.15	0.26	0.25	0.26	0.27
Cr	0.00	0.00	0.00	0.00	0.00	0.00	0.00	0.00	0.00	0.00
Fe^{2+}	0.32	0.32	0.32	0.32	0.31	0.32	0.36	0.35	0.36	0.36
Mn	0.01	0.01	0.01	0.01	0.01	0.01	0.01	0.01	0.01	0.01
Ni	0.00	0.00	0.00	0.00	0.00	0.00	0.00	0.00	0.00	0.00
Mg	0.63	0.64	0.65	0.65	0.66	0.65	0.56	0.57	0.57	0.56
Ca	0.91	0.91	0.91	0.92	0.91	0.91	0.90	0.90	0.89	0.89
Na	0.10	0.09	0.09	0.08	0.09	0.09	0.11	0.12	0.11	0.12
Total	4.06	4.05	4.05	4.04	4.05	4.05	4.07	4.07	4.06	4.07
Mg#	0.66	0.66	0.67	0.67	0.68	0.67	0.61	0.62	0.61	0.61

* Total Fe as FeO

Table 3. Representative chemical analyses and structural formulae (O^{2-} = 6) of clinopyroxene megacryst DL3310 from the Ostrzyca Proboszczowicka (see Fig. 6c).

Analysis no.	5 / 1 .	6 / 1 .	7 / 1 .	8 / 1 .	9 / 1 .	11 / 1 .	12 / 1 .	13 / 1 .	14 / 1 .	15 / 1 .
SiO_2	48.43	50.22	50.44	50.33	50.12	50.49	50.36	50.60	49.21	48.95
TiO_2	1.48	0.84	0.85	0.78	0.85	0.89	0.85	0.84	1.18	1.31
Al_2O_3	4.99	3.24	3.22	3.16	3.28	2.98	3.12	3.18	4.38	4.73
Cr_2O_3	0.00	0.00	0.00	0.00	0.01	0.01	0.05	0.00	0.01	0.01
FeO*	10.58	9.72	9.68	9.85	9.73	9.48	9.74	9.85	10.33	10.50
MnO	0.22	0.28	0.30	0.26	0.30	0.25	0.27	0.24	0.25	0.26
NiO	0.00	0.01	0.03	0.03	0.01	0.01	0.00	0.02	0.00	0.00
MgO	10.35	11.35	11.48	11.40	11.35	11.61	11.33	11.38	10.69	10.64
CaO	21.84	22.05	22.36	22.43	22.22	22.56	22.26	22.43	21.91	21.90
Na_2O	1.64	1.27	1.25	1.30	1.30	1.06	1.39	1.31	1.64	1.53
Total	99.53	98.99	99.60	99.53	99.16	99.33	99.36	99.86	99.61	99.86
Si	1.85	1.91	1.91	1.91	1.91	1.91	1.91	1.91	1.87	1.86
Ti	0.04	0.02	0.02	0.02	0.02	0.03	0.02	0.02	0.03	0.04
Al	0.22	0.15	0.14	0.14	0.15	0.13	0.14	0.14	0.20	0.21
Cr	0.00	0.00	0.00	0.00	0.00	0.00	0.00	0.00	0.00	0.00
Fe^{2+}	0.34	0.31	0.31	0.31	0.31	0.30	0.31	0.31	0.33	0.33
Mn	0.01	0.01	0.01	0.01	0.01	0.01	0.01	0.01	0.01	0.01
Ni	0.00	0.00	0.00	0.00	0.00	0.00	0.00	0.00	0.00	0.00
Mg	0.59	0.64	0.65	0.64	0.64	0.66	0.64	0.64	0.61	0.60
Ca	0.89	0.90	0.91	0.91	0.91	0.92	0.91	0.91	0.89	0.89
Na	0.12	0.09	0.09	0.10	0.10	0.08	0.10	0.10	0.12	0.11
Total	4.06	4.04	4.04	4.05	4.04	4.03	4.04	4.04	4.06	4.06
Mg#	0.64	0.68	0.68	0.67	0.68	0.69	0.67	0.67	0.65	0.64

* Total Fe as FeO

Table 4. Representative chemical analyses and structural formulae (O^{2-} = 6) of fringes of clinopyroxene megacrysts from the Ostrzyca Proboszczowicka.

sample	DL3304				DL3307			DL3308	DL3309			DL3310		
Analysis no.	113 / 1 .	117 / 1 .	118 / 1 .	119 / 1 .	66 / 1 .	67 / 1 .	68 / 1 .	26 / 1 .	8 / 1 .	17 / 1 .	22 / 1 .	1 / 1 .	2 / 1 .	17 / 1 .
SiO_2	49.00	48.63	41.95	45.39	43.20	46.05	47.36	47.67	50.32	48.69	47.09	44.11	50.68	50.90
TiO_2	1.44	1.96	4.55	3.28	3.66	2.57	1.98	1.92	1.25	1.46	2.09	3.53	1.21	1.01
Al_2O_3	5.24	4.38	9.76	7.69	9.07	6.85	6.04	6.30	3.59	5.25	7.26	8.47	3.87	3.95
Cr_2O_3	0.73	0.05	0.02	0.00	0.18	0.37	0.68	1.08	0.58	0.09	0.00	0.03	0.58	0.77
FeO*	4.95	6.05	7.98	7.04	7.33	6.12	5.56	5.23	4.65	7.31	7.10	7.17	4.56	4.30
MnO	0.06	0.09	0.09	0.14	0.10	0.12	0.06	0.11	0.07	0.11	0.12	0.08	0.08	0.08
NiO	0.01	0.03	0.02	0.02	0.02	0.03	0.03	0.04	0.02	0.00	0.00	0.02	0.06	0.03
MgO	14.57	14.16	10.66	11.93	11.70	13.11	13.75	13.78	15.20	12.72	12.49	11.84	15.25	15.41
CaO	22.96	23.23	23.04	22.63	23.54	23.47	23.48	23.19	23.33	22.29	22.49	23.43	23.58	23.33
Na_2O	0.47	0.13	0.25	0.73	0.46	0.40	0.52	0.49	0.37	1.02	0.81	0.44	0.39	0.43
Total	99.44	98.72	98.33	98.83	99.24	99.12	99.45	99.79	99.37	98.95	99.47	99.13	100.26	100.21
Si	1.82	1.83	1.62	1.72	1.65	1.74	1.78	1.78	1.87	1.84	1.77	1.68	1.87	1.87
Ti	0.04	0.06	0.13	0.09	0.10	0.07	0.06	0.05	0.03	0.04	0.06	0.10	0.03	0.03
Al	0.23	0.19	0.44	0.34	0.41	0.30	0.27	0.28	0.16	0.23	0.32	0.38	0.17	0.17
Cr	0.02	0.00	0.00	0.00	0.01	0.01	0.02	0.03	0.02	0.00	0.00	0.00	0.02	0.02
Fe^{2+}	0.15	0.19	0.26	0.22	0.23	0.19	0.17	0.16	0.14	0.23	0.22	0.23	0.14	0.13
Mn	0.00	0.00	0.00	0.00	0.00	0.00	0.00	0.00	0.00	0.00	0.00	0.00	0.00	0.00
Ni	0.00	0.00	0.00	0.00	0.00	0.00	0.00	0.00	0.00	0.00	0.00	0.00	0.00	0.00
Mg	0.81	0.80	0.61	0.67	0.66	0.74	0.77	0.77	0.84	0.72	0.70	0.67	0.84	0.84
Ca	0.91	0.94	0.95	0.92	0.96	0.95	0.94	0.93	0.93	0.90	0.91	0.95	0.93	0.92
Na	0.03	0.01	0.02	0.05	0.03	0.03	0.04	0.04	0.03	0.07	0.06	0.03	0.03	0.03
Total	4.03	4.02	4.04	4.04	4.06	4.04	4.04	4.03	4.02	4.04	4.04	4.05	4.02	4.02
Mg#	0.84	0.81	0.70	0.75	0.74	0.79	0.82	0.82	0.85	0.76	0.76	0.75	0.86	0.86

* Total Fe as FeO

Table 5. Trace element contents (ppm) in clinopyroxene megacryst DL3307 from the Ostrzyca Proboszczowicka.

Analysis no.	1	2	3	4	5	6	7	8	9	10
Rb	0.00	0.15	0.08	0.00	0.23	0.01	0.02	0.01	0.25	0.14
Ba	0.13	2.26	1.57	0.07	9.34	0.24	0.62	0.06	3.55	3.72
Th	0.34	0.09	0.07	0.05	0.11	0.05	0.04	0.05	0.19	0.11
U	0.02	0.02	0.01	0.01	0.03	0.01	0.01	0.01	0.03	0.04
Nb	1.77	2.15	1.82	1.23	1.98	1.18	1.33	1.27	3.28	2.44
Ta	0.38	0.69	0.68	0.41	0.50	0.41	0.47	0.43	1.10	0.89
La	12.63	6.21	6.10	5.38	6.36	5.20	5.29	5.45	7.03	6.74
Ce	37.93	23.71	21.19	21.17	21.44	20.51	20.14	21.34	25.02	24.18
Pb	0.09	0.12	0.24	0.11	0.17	0.12	0.49	0.13	0.24	0.17
Pr	6.19	4.41	4.55	4.08	4.35	3.94	3.96	3.97	4.77	4.64
Sr	147.35	255.23	251.57	243.36	265.36	246.25	248.26	251.59	263.67	255.24
Nd	29.98	21.87	22.33	20.29	21.42	19.58	19.75	19.66	23.33	22.74
Zr	180.70	713.84	819.22	586.70	642.66	579.60	717.85	646.41	901.51	907.80
Hf	7.23	26.38	30.01	20.79	22.74	20.16	25.64	22.62	33.86	33.43
Sm	7.19	5.60	5.82	5.22	5.45	5.14	5.15	5.09	5.94	5.89
Eu	2.34	1.86	1.96	1.78	1.83	1.69	1.70	1.68	1.96	1.95
Ti	16535.16	7066.67	6189.36	5107.13	5454.63	5115.88	5364.28	5004.74	8541.70	7423.97
Gd	6.59	4.86	5.14	4.53	4.73	4.38	4.54	4.38	5.12	5.01
Dy	4.38	3.36	3.60	3.21	3.26	3.06	3.18	3.02	3.49	3.44
Y	16.41	11.21	12.32	11.01	11.41	10.60	10.92	10.37	11.74	11.70
Ho	0.71	0.52	0.57	0.50	0.51	0.48	0.50	0.47	0.54	0.54
Er	1.55	1.12	1.29	1.10	1.13	1.06	1.11	1.08	1.19	1.17
Yb	1.04	0.88	1.04	0.91	0.93	0.84	0.94	0.89	0.89	0.90
Lu	0.14	0.14	0.17	0.15	0.16	0.14	0.16	0.15	0.15	0.15

Table 6. Trace element contents (ppm) in clinopyroxene megacryst DL3308 from the Ostrzyca Proboszczowicka.

Analysis no.	1	2	3	4	5	6	7	8
Rb	0.14	0.15	0.01	0.00	4.93	0.00	0.19	0.05
Ba	2.91	5.19	0.11	0.05	114.58	0.12	3.04	0.06
Th	0.07	0.07	0.04	0.04	1.38	0.08	0.13	0.07
U	0.01	0.02	0.02	0.01	0.41	0.01	0.02	0.01
Nb	1.64	1.46	1.21	1.13	14.87	3.01	3.64	2.64
Ta	0.58	0.42	0.46	0.44	1.14	1.38	1.52	1.16
La	5.85	5.65	5.29	5.29	10.62	7.01	7.46	6.49
Ce	23.63	22.46	22.10	22.34	32.59	28.86	30.09	26.94
Pb	0.20	0.18	0.23	0.12	0.93	0.12	0.24	0.13
Pr	3.90	3.63	3.65	3.66	4.61	4.75	4.96	4.40
Sr	262.57	251.77	237.86	236.21	358.80	251.31	252.20	252.22
Nd	21.11	19.78	20.09	20.29	23.33	26.18	27.10	24.02
Zr	611.34	492.47	625.45	639.60	578.82	932.36	977.83	827.58
Hf	22.41	18.46	24.18	24.78	20.97	34.71	36.68	31.68
Sm	5.45	5.12	5.19	5.33	5.71	6.77	6.97	6.15
Eu	1.64	1.56	1.59	1.60	1.74	2.04	2.11	1.90
Ti	7123.57	5757.93	6074.96	5795.59	6260.89	11492.21	12278.19	10736.40
Gd	4.79	4.62	4.71	4.75	5.17	6.01	6.11	5.47
Dy	3.30	3.19	3.32	3.33	3.58	4.17	4.22	3.80
Y	11.06	10.64	10.87	11.23	12.47	13.49	14.09	12.54
Ho	0.50	0.47	0.49	0.49	0.55	0.61	0.63	0.57
Er	1.28	1.18	1.22	1.25	1.40	1.53	1.58	1.39
Yb	0.85	0.80	0.83	0.87	0.94	0.97	1.01	0.87
Lu	0.13	0.13	0.12	0.14	0.14	0.14	0.14	0.13

Table 7. Trace element contents (ppm) in fringes of clinopyroxene megacrysts from the Ostrzyca Proboszczowicka.

Analysis no.	DL3303	DL3307	DL3308	Dl3309
Rb	0.21	0.00	0.43	0.15
Ba	3.30	0.13	8.86	3.46
Th	0.33	0.34	0.29	0.17
U	0.04	0.02	0.06	0.03
Nb	2.38	1.77	2.30	1.50
Ta	0.48	0.38	0.31	0.26
La	11.04	12.63	7.11	10.34
Ce	36.29	37.93	23.29	34.51
Pb	0.26	0.09	0.13	0.13
Pr	5.12	6.19	3.37	5.76
Sr	136.32	147.35	133.60	214.99
Nd	25.42	29.98	17.84	27.22
Zr	190.42	180.70	112.45	191.34
Hf	8.20	7.23	4.83	7.50
Sm	6.56	7.19	4.47	6.46
Eu	2.03	2.34	1.39	2.06
Ti	18440.75	16535.16	12501.23	7510.57
Gd	6.39	6.59	4.39	5.70
Dy	4.49	4.38	3.14	3.84
Y	18.41	16.41	12.29	14.49
Ho	0.74	0.71	0.51	0.63
Er	1.72	1.55	1.33	1.38
Yb	1.13	1.04	0.81	0.92
Lu	0.16	0.14	0.11	0.13

Table 8. Representative chemical analyses, structural formulae (O^{2-} = 26) and trace element contents (ppm) in apatite inclusions in clinopyroxene megacryst DL3302 from the Ostrzyca Proboszczowicka.

Analysis no.	1	2	3	4	5	6
CaO	53.97	54.33	54.38			
SrO	0.43	0.47	0.48			
FeO	0.05	0.12	0.05			
MgO	0.06	0.10	0.08			
La_2O_3	0.10	0.07	0.07			
Ce_2O_3	0.13	0.23	0.21			
P_2O_5	40.56	40.22	40.60			
SiO_2	0.55	0.59	0.55			
Cl	0.12	0.09	0.06			
F	0.94	1.22	1.10			
Total	96.91	97.43	97.57			
O=F.Cl	0.42	0.53	0.48			
Total	96.48	96.90	97.09	LACK OF MICROPROBE DATA		
Ca	9.89	9.95	9.96			
Sr	0.04	0.05	0.05			
Fe	0.01	0.02	0.01			
Mg	0.02	0.02	0.02			
La	0.01	0.00	0.00			
Ce	0.01	0.01	0.01			
P	5.87	5.82	5.88			
Si	0.09	0.10	0.09			
Cl	0.04	0.03	0.02			
F	0.51	0.66	0.60			
OH	0.46	0.31	0.39			
Total	16.93	16.98	17.02			
Rb	0.03	0.03	0.05	0.03	0.05	0.03
Ba	17.19	18.02	18.24	20.75	20.27	17.58
Th	28.91	29.81	30.53	28.16	29.33	27.90
U	4.48	4.35	4.49	4.18	4.29	4.15
Nb	1.35	1.47	1.59	1.41	1.46	1.34
Ta	0.04	0.04	0.05	0.04	0.04	0.04
La	582.61	565.81	569.34	553.24	564.41	556.45
Ce	1487.92	1434.76	1436.20	1393.95	1416.64	1422.70
Pb	0.63	0.67	0.65	0.58	0.64	0.63
Pr	200.07	192.20	193.39	186.88	191.06	189.18
Sr	3389.22	3411.78	3390.85	3502.86	3387.68	3425.04
Nd	882.25	853.77	854.51	825.21	847.37	834.28
Zr	29.24	28.32	29.38	27.27	28.18	27.14

Continued on next page.

Hf	0.16	0.17	0.17	0.14	0.16	0.14
Sm	152.35	147.22	148.14	142.92	146.19	143.08
Eu	42.23	40.61	40.83	39.38	40.29	39.68
Ti	18.63	18.54	18.66	17.97	18.50	17.17
Gd	119.11	114.58	115.40	111.99	114.00	111.48
Dy	59.78	57.28	57.63	55.66	57.00	55.66
Y	219.96	210.10	213.07	207.14	211.86	207.88
Ho	8.90	8.56	8.61	8.28	8.48	8.27
Er	18.07	17.20	17.45	16.90	17.26	16.75
Yb	8.67	8.19	8.40	8.07	8.30	7.93
Lu	0.96	0.91	0.92	0.88	0.90	0.88

Table 9. Representative chemical analyses, structural formulae (O^{2-} = 26) and trace element contents (ppm) in apatite inclusions in clinopyroxene megacryst DL3310 from the Ostrzyca Proboszczowicka.

Analysis no.	1	2	3	4
CaO	53.86	54.00	54.40	54.36
SrO	0.32	0.44	0.39	0.43
FeO	0.04	0.05	0.05	0.18
MgO	0.05	0.07	0.06	0.12
La_2O_3	0.05	0.09	0.06	0.04
Ce_2O_3	0.15	0.12	0.14	0.13
P_2O_5	40.20	40.50	40.38	40.22
SiO_2	0.49	0.50	0.44	0.49
Cl	0.09	0.09	0.13	0.08
F	0.92	0.98	0.87	1.40
Total	96.17	96.84	96.91	97.44
O=F.Cl	0.41	0.43	0.40	0.61
Total	95.76	96.40	96.51	96.83
Ca	9.87	9.89	9.96	9.96
Sr	0.03	0.04	0.04	0.04
Fe	0.01	0.01	0.01	0.03
Mg	0.01	0.02	0.01	0.03
La	0.00	0.01	0.00	0.00
Ce	0.01	0.01	0.01	0.01
P	5.82	5.86	5.84	5.82
Si	0.08	0.09	0.08	0.08
Cl	0.03	0.02	0.04	0.02
F	0.50	0.53	0.47	0.75
OH	0.48	0.44	0.49	0.22
Total	16.83	16.92	16.96	16.97
Rb	0.03	0.44	0.04	0.03

Continued on next page.

Ba	20.38	57.56	23.44	20.70
Th	23.83	24.46	25.48	25.98
U	3.61	4.11	3.93	3.99
Nb	1.07	3.39	1.30	1.38
Ta	0.03	0.10	0.04	0.04
La	504.82	506.51	521.51	531.95
Ce	1277.39	1274.10	1317.16	1331.65
Pb	0.57	9.48	0.65	0.61
Pr	170.56	169.91	175.46	178.53
Sr	3126.86	3184.14	3439.94	3346.89
Nd	757.50	754.96	779.57	789.82
Zr	24.15	29.94	25.84	26.69
Hf	0.15	0.23	0.16	0.17
Sm	131.91	132.51	135.27	136.71
Eu	36.38	36.56	37.75	38.08
Ti	18.64	52.34	18.59	17.54
Gd	104.56	105.33	109.57	110.38
Dy	51.84	51.83	53.67	54.23
Y	189.33	189.54	195.78	198.04
Ho	7.64	7.74	8.04	8.08
Er	15.63	15.80	16.30	16.50
Yb	7.69	7.70	8.00	8.18
Lu	0.84	0.84	0.87	0.87

Host basanite

The basanite from Ostrzyca Proboszczowicka contains 12–13% of normative olivine (Szumowska 2013). It is continuously enriched from HREE to LREE (La_N/Lu_N=33.23–35.23, Table 10).

The basanite consists of phenocrysts of clinopyroxene and olivine occurring in groundmass formed of olivine, clinopyroxene, plagioclase and nepheline. Phenocrysts of clinopyroxene (max. 1.2 mm in diameter) are euhedral to subhedral, light yellow, pleochroic. Some of them have green cores or cores with sieve texture — with large amount of small inclusions — covered by clear darker rims. Their composition varies from aluminian diopside to aluminian-titanian-subsilicic diopside (Figure 4, Table 11). Some phenocrysts reveal the oscillatory zoning. Olivine grains (typically 1 mm, maximally 2.7 mm) are subhedral to anhedral. Some are fractured, brown to red in color. The forsterite content varies from 84.35% in cores to 80.38 mole % in rims. The Ca content (1286–1808 ppm) is negatively correlated with that of Ni (1069–1697 ppm).

The groundmass clinopyroxene has the composition of subsilicic diopside, enriched in Ca (1.07 a pfu), whereas the groundmass olivine (Fo 63.11 to 84.07 mole % contains from 1422 to 6018 ppm of Ca and from 809 to 2090 ppm) of Ni.

The colourless, euhedral to subhedral grains of nepheline are up to 70 μm long. Euhedral laths of plagioclase (56.2 to 58.5 mole % of anorthite) are from 0.1 to 0.2 mm long. Spinel grains are usually 0.01 mm in diameter, some reach up to 0.8 mm.

Table 10. Chemical composition of host basanite from Ostrzyca Proboszczowicka Hill.

Sample no.	OS-1	OS-2	OS-3	OS-5AR	OS-5BR
weight percents					
SiO_2	44.61	42.11	42.19	41.84	41.89
TiO_2	2.80	2.73	2.71	2.73	2.72
Al_2O_3	12.63	11.81	11.86	11.75	11.77
Fe_2O_3	12.72	12.52	12.38	12.47	12.41
MnO	0.19	0.18	0.18	0.18	0.18
MgO	12.53	11.69	11.94	12.41	12.31
CaO	13.24	12.87	12.61	12.67	12.63
Na_2O	3.18	3.08	2.98	3.00	3.06
K_2O	1.19	1.11	1.20	1.11	1.09
P_2O_5	1.03	0.99	0.98	0.98	0.96
Total	104.12	99.08	99.02	99.13	99.03
Mg#	0.66	0.65	0.66	0.66	0.66
ppm					
Ni	268.00	277.90	266.60	288.30	288.80
Co	44.70	45.70	44.70	46.60	46.40
Cr	422.10	435.90	414.60	445.00	446.60
V	270.20	271.50	266.20	272.20	268.90

Table 11. Representative chemical analyses and structural formulae (O^{2-} = 6) of groundmass clinopyroxene from sample DL3308 from the Ostrzyca Proboszczowicka.

Analysis no.	1 / 1 .	2 / 1 .	3 / 1 .	4 / 1 .	5 / 1 .
SiO_2	41.56	45.83	42.62	48.71	41.22
TiO_2	4.69	2.72	4.15	1.88	3.51
Al_2O_3	10.52	7.21	10.30	4.73	7.97
Cr_2O_3	0.01	0.58	0.00	0.11	0.00
FeO*	7.64	6.39	7.93	5.98	7.62
MnO	0.15	0.07	0.12	0.07	0.13
NiO	0.04	0.04	0.00	0.03	0.00
MgO	10.20	12.79	10.73	14.38	10.44
CaO	23.32	23.64	22.85	23.58	25.21
Na_2O	0.66	0.46	0.73	0.35	0.60
Total	98.79	99.74	99.46	99.86	96.74
Si	1.60	1.72	1.62	1.82	1.63

Continued on next page.

Ti	0.14	0.08	0.12	0.05	0.10
Al	0.48	0.32	0.46	0.21	0.37
Cr	0.00	0.02	0.00	0.00	0.00
Fe^{2+}	0.25	0.20	0.25	0.19	0.25
Mn	0.00	0.00	0.00	0.00	0.00
Ni	0.00	0.00	0.00	0.00	0.00
Mg	0.58	0.72	0.61	0.80	0.62
Ca	0.96	0.95	0.93	0.94	1.07
Na	0.05	0.03	0.05	0.03	0.05
Total	4.05	4.05	4.06	4.04	4.10
Mg#	0.70	0.78	0.71	0.81	0.71

* Total Fe as FeO

Discussion and conclusive remarks

The megacrysts of clinopyroxene have been reported from many occurrences of alkali basalts belonging to the Central European Volcanic Province (e.g. Liotard et al. 1988; Shaw and Eyzaguirre 2000; Ulianov et al. 2007; Woodland and Jugo 2007). Typically, clinopyroxene megacrysts are precipitates from mafic magma crystalizing at either crustal or mantle depths. To establish relationship between the Ostrzyca megacrysts and their host basanite, we have calculated the FeO/MgO ratio of megacryst's parental magma. We used the equation Kd = $[(FeO/MgO)_{Cpx}$*$(MgO/FeO)_{liq}]$, assuming the ratio of Fe^{3+}/Fe^{2+} = 0.20 (Woodland and Jugo 2007) and used the partition coefficients ranging from 0.28 to 0.33 (Putirka et al. 1996; Woodland and Jugo 2007). The obtained results show that the megacrysts did not crystallize from the basanite, in which they now occur (Table 12), but from the magma of lower Mg/(Mg+Fe) ratio. Moreover, the calculations show that the clinopyroxenitic fringes crystallized directly from the host basanite. That is also suggested by their chemical composition, identical to that of basanite groundmass clinopyroxene.

Table 12. Calculated ratio $(MgO/FeO)_{liq}$ for the hypothetical parent magma, which were formed the megacrysts and the fringe.

	$(MgO/FeO)_{liq}$ for the megacrysts	$(MgO/FeO)_{liq}$ for the fringes
DL3302	0.32-0.47	0.71-1.21
DL3303	0.40-0.50	0.81-0.96
DL3304	0.38-0.58	0.42-1.26
DL3307	0.33-0.47	0.56-1.02
DL3308	0.31-0.48	0.56-1.10
DL3309	0.36-0.50	0.61-1.35
DL3310	0.34-0.51	0.58-1.48
basanite	1.30-1.38	
phenocrysts	1.67-3.01	

All of the investigated megacrysts plot in the field of "granulites and inclusions in basalts" in the Al ^{IV}–Al ^{VI} diagram (Aoki and Shiba 1973; Figure 9).

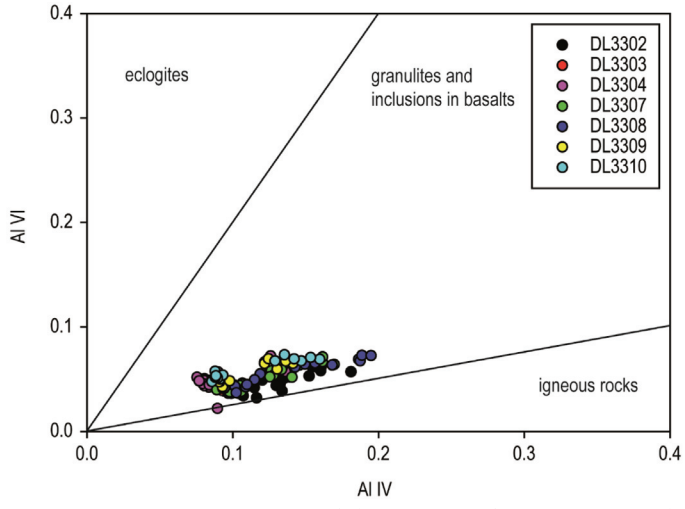

Figure 9. Points representing megacrysts of clinopyroxene from Ostrzyca Proboszczowicka in the AlIV – AlVI diagram of Aoki and Shiba (1973)

This may suggest their high-pressure origin. However, the partitioning of the aluminium on the tetrahedral and octahedral sites does not indicate the high-pressure conditions of their crystallization. The Al^{VI}/Al^{IV} is < 1 (Table 13), which suggests crustal conditions of origin, since the values $Al^{VI}/Al^{IV} \geq 1$ are characteristic for mantle-derived clinopyroxene (Cvetković et al. 2012). The clinopyroxene megacrysts from Ostrzyca Proboszczowicka are similar, in terms of major and trace elements, to the "type 2" of megacrysts described by Woodland and Jugo (2007) from basanites of Mont Briançon and Marais de Limagne in Massif Central. Since the latter crystallized under crustal conditions (P = 3–4 kbar) we assume, by analogy, that the Ostrzyca megacrysts are also of crustal origin.

Table 13. The Al ^{VI}/Al ^{IV} ratio in the megacrysts and their fringes.

	Al ^{VI}/Al ^{IV} in the megacrysts	Al ^{VI}/Al ^{IV} in the fringes
DL3302	0.28-0.44	0.12-0.25
DL3303	0.35-0.50	0.21
DL3304	0.25-0.69	0.16-0.61
DL3307	0.36-0.51	0.15-0.19
DL3308	0.36-0.46	0.17-0.24
DL3309	0.46-0.62	0.15-0.43
DL3310	0.43-0.66	0.18-0.32

The calculation of REE contents in the parental melt of megacrysts (partition coefficients of Hart and Dunn 1993) shows that megacrysts crystallized from a melt

similar to the host basanite (Figure 10). This suggests that the megacrysts crystallized from alkaline basaltic magma subjected to local differentiation, which (1) enabled the crystallization of apatite and (2) lowered its Mg/(Mg+Fe) ratio, which is visible in the megacryst composition. We speculate that the megacrysts settled to form an unconsolidated cumulate in the transitional magma chamber or temporarily blocked magma channel. This cumulate was entrained into the subsequent magma pulse and dispersed into individual grains occurring now in the basanite.

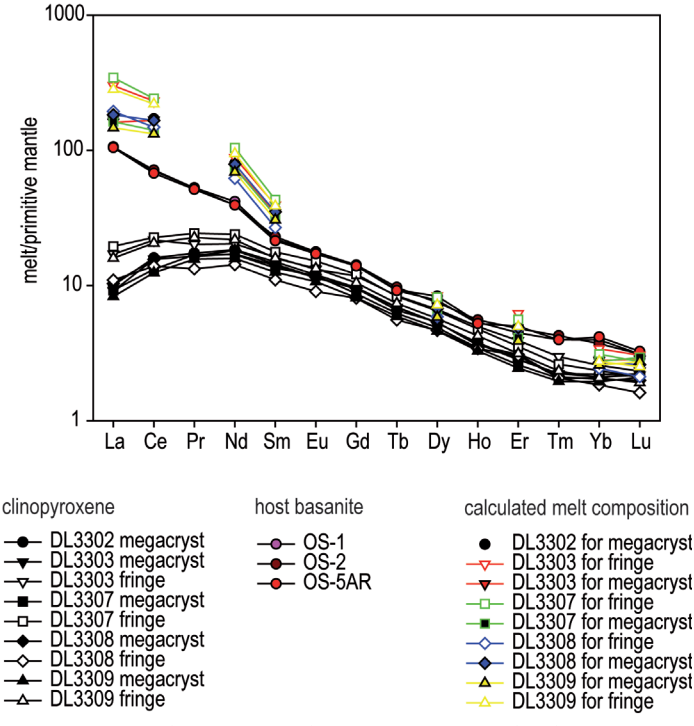

Figure 10. Primitive mantle (McDonough & Sun 1995) normalized REE patterns calculated for the parental melt coexisting in equilibrium with the clinopyroxene megacrysts. For comparison the REE patterns of host basanite, megacrysts and their reaction fringes are shown

Acknowledgments

This study is a summary of MSc thesis of the first author and was possible thanks to the project NCN 2011/03/B/ST10/06248 of Polish National Centre for Science to Magdalena Matusiak-Małek. We express our thanks to Robert Anczkiewicz (ING PAN, Kraków) for his invaluable help during LA ICP-MS analyses.

References

Aoki K. , I. Shiba. 1973. Pyroxenes from lherzolite inclusions of Itinomegata. Japan. *Lithos*, 6, pp. 41–51.

Bakun–Czubarow N., A. Białowolska. 2001. Clinopyroxene- and olivine megacrysts from basaltoids of the Lądek Zdrój area (SW Poland). *Polskie Towarzystwo Mineralogiczne – Prace Specjalne*, 19, pp. 23–25.

Białowolska A. 1980. Geochemiczna charakterystyka niektórych bazaltoidów Dolnego Śląska i ich ultramafitowych enklaw. *Archiwum Mineralogiczne*, 36, pp. 107–170.

Birkenmajer K., Z. Pécskay, J. Grabowski, M.W. Lorenc, P. Zagożdżon. 2007. Radiometric dating of the Tertiary volcanics in Lower Silesia, Poland. V. K-Ar and paleomagnetic data from Late Oligocene to Early Miocene basaltic rocks of the North-Sudetic Depression. *Annales Societatis Geologorum Poloniae*, 77, pp. 1–16.

Cvetković V., S. Erić, M. Radivojević, K. Šarić. 2012. Cognate clinopyroxene from Paleogene mantle xenoliths-bearing basanite lavas (East Serbia, SE Europe): the role of dissolution of mantle orthopyroxene. *Mineralogy and Petrology*, 106, pp. 131–150.

Hart S.R., T. Dunn. 1993. Experimental cpx/melt partitioning of 24 trace elements. *Contributions to Mineralogy and Petrology*, 113, pp. 1–8.

Kozłowska-Koch M. 1976. Petrography of ultramafic nodules in basaltoids from the environs of Lądek (Sudetes). *Bulletin de l'Académie Polonaise des Sciences, Série Sciences de la Terre*, 24, pp. 67–76.

Kozłowska-Koch M. 1981. Petrography of ultramafic nodules in the nephelinites from Księginki near Lubań (Lower Silesia). *Archiwum Mineralogiczne*, 37, pp. 33–59.

Liotard J.M., D. Briot, P. Boivin. 1988. Petrological and geochemical relationships between pyroxene megacrysts and associated alkali-basalts from Massif Central (France). *Contributions to Mineralogy and Petrology*, 98, pp. 81–90.

Matusiak-Małek M. 2010. Peridotitic xenoliths from the Cenozoic lavas of the Złotoryja, Jawor and Lądek Zdrój vicinities (Lower Silesia). PhD Thesis, Faculty of Earth Sciences and Environmental Management, University of Wrocław.

Matusiak-Małek M., J. Puziewicz, T. Ntaflos, M. Grégoire, M. Benoit, A. Klügel. 2014. Two contrasting lithologies in off-rift subcontinental lithospheric mantle beneath Central Europe — the Krzeniów (SW Poland) case study. *Journal of Petrology*, 55, 1799–1828.

Morimoto N. 1989. Nomenclature of pyroxenes. *Canadian Mineralogist*, 27, pp. 143–156.

McDonough W.F., S.-S. Sun. 1995. The composition of the Earth. *Chemical Geology*, 120, pp. 223–253.

Milewicz J., W. Kozdrój. 1995. Szczegółowa mapa geologiczna Sudetów 1:25000. Arkusz Proboszczów. Wydawnictwo Kartograficzne Polskiej Agencji Ekologicznej S.A.

Putirka K., M. Johnson, R. Kinzler, J. Longhi, D. Walker. 1996. Thermobarometry of mafic igneous rocks based on clinopyroxene-liquid equilibria, 0-30 kbar. *Contributions to Mineralogy and Petrology*, 123, pp. 92–108.

Puziewicz J., J. Koepke, M. Grégoire, T. Ntaflos, M. Matusiak-Małek. 2011. Lithospheric mantle modification during Cenozoic rifting in Central Europe: Evidence from the Księginki nephelinite (SW Poland) xenolith suite. *Journal of Petrology*, 52, pp. 2107–2145.

Puziewicz J., M. Matusiak-Małek, T. Ntaflos, M. Grégoire, A. Kukuła. 2015. Subcontinental lithospheric mantle beneath Central Europe. *International Journal of Earth Sciences*, in press.

Sawicki L. 1995. Geological map of Lower Silesia with adjacent Czech and German territories (without Quaternary deposits), 1:100000. Państwowy Instytut Geologiczny.

Shaw C.S.J., J. Eyzaguirre. 2000. Origin of megacrysts in the mafic alkaline lavas of the West Eifel volcanic field, Germany. *Lithos*, 50, pp. 75–95.

Szumowska M. 2013. Geologia i petrologia kenozoicznych skał wulkanicznych góry Ostrzyca na Pogórzu Kaczawskim. MSc Thesis, Faculty of Earth Sciences and Environmental Management, University of Wrocław.

Szumowska M., M. Awdankiewicz, E.H. Christiansen. 2013. Geology and petrology of Cenozoic volcanic rocks of Ostrzyca Hill in the Kaczawa Foothills, SW Poland. *Mineralogia – Special Papers*, 41, pp. 88.

Ulianov A., O. Müntener, P. Ulme, T. Pettke. 2007. Entrained macrocryst minerals as a key to the source region of olivine nephelinites: Humberg, Kaiserstuhl, Germany. *Journal of Petrology*, 48, pp. 1079–1118.

Ulrych J., E. Pivec, M. Lang, K. Balogh, V. Kropáček. 1999. Cenozoic intraplate volcanic rock series of the Bohemian Massif: a review. *Geolines*, 9, pp. 123–129.

Ulrych J., J. Dostal, J. Adamovič, E. Jelínek, P. Špaček, E. Hegner, K. Balogh. 2011. Recurrent Cenozoic volcanic activity in the Bohemian Massif (Czech Republic). *Lithos*, 123, pp. 133–144.

Wilson M., H. Downes. 2006. Tertiary-Quaternary intra-plate magmatism in Europe and its relationship to mantle dynamics. In: Gee D.G. and Stephenson R. (eds.) European lithosphere dynamics. Geological Society of London Memoir 32. London: Geological Society of London, pp. 147–166.

Woodland A.B., P. Jugo. 2007. A complex magmatic system beneath the Devès volcanic field, Massif Central, France: evidence from clinopyroxene megacrysts. *Contributions to Mineralogy and Petrology*, 153, pp. 719–731.